



CERN-EP-2019-xxx  
April 27, 2020

## Long range correlations and their event scale dependence in high multiplicity pp collisions at $\sqrt{s} = 13$ TeV

### Abstract

The observed azimuthal modulations of long-range correlations in pseudorapidity in small systems like pp or p-Pb collisions show strikingly similar features to those seen in heavy ion collisions. Many theoretical approaches to interpreting this effect have been developed. However, it is still unclear whether these long-range correlations are due to final or initial state effects. To further investigate these effects, we studied long-range correlations as a function of transverse momentum in very high multiplicity pp collisions at  $\sqrt{s} = 13$  TeV, collected with the high multiplicity event trigger during 2016 and 2017 with ALICE. In this talk, we present the near-side per-trigger yield at large pseudorapidity separation (ridge yield) as a function of transverse momentum in pp collisions at  $\sqrt{s} = 13$  TeV. The results are compared to previous measurements from CMS experiments. In addition, we present the ridge yield in events where harder fragmentation processes are present, to explore possible physical origins of long-range correlations.

## 1 Introduction

Measurements of two-particle angular correlations are typically performed in terms of two dimensional  $\Delta\eta - \Delta\phi$  correlation functions, where  $\eta$  is the pseudorapidity and  $\phi$  is the azimuthal angle. Of particular interest in studies of possible novel collective effects is the long-range structure of two-particle correlation functions, in which the effects of known sources such as resonance decays and fragmentation of high-momentum partons are known to be small. In most Monte Carlo (MC) event generators for proton-proton (pp) collisions, the typical sources of such long-range correlations are momentum conservation and away-side ( $\Delta\phi \approx \pi$ ) jet correlations. The enhancement in the associated yield of two-particle correlations at small relative azimuthal angle ( $\Delta\phi$ ) that extends over a long-range of relative pseudorapidity ( $\Delta\eta$ ), is dubbed “ridge” due to its shape in  $\Delta\eta - \Delta\phi$  plot. The shape of these  $\Delta\phi$  correlations can be studied via a Fourier decomposition [1, 2]. The second and third order terms are the dominant harmonic coefficients  $v_n$ . The  $v_n$  coefficients can be related to the collision geometry and density fluctuations of the colliding nuclei [3–5] and to the transport properties of the QGP in hydrodynamic models [6, 7].

Strong collectivity observed in the azimuthal correlations of particles emitted over a wide pseudorapidity range, in high-energy nucleus-nucleus collisions at RHIC [8–11] and LHC [12–14], has indicated the formation of a strongly interacting quark gluon plasma (QGP) matter, which exhibits hydrodynamic behavior [15]. The recent efforts are nowadays focused on constrainig the transport properties of the QGP in hydrodynamic models [6, 7] along with few advanced experimental works [16–19]. In recent years similar long-range collective azimuthal correlations are also observed for small systems with high final-state particle multiplicity such as proton-proton (pp) [20–23] proton-nucleus (pA) [24], and lighter nucleus-nucleus systems [25], revealing strong indications for collective flow with hydrodynamic characteristics even in small systems, even though the volume and lifetime of the medium produced are expected to be small.

The ridge structures in high-multiplicity pp and pPb events have been attributed to mechanisms that involve initial-state effects, such as gluon saturation [26] and colour connections [27] forming along the longitudinal direction and final-state effects, such as parton-induced interactions [28], and collective effects arising in a high-density system possibly formed in these collisions [29]. As a natural choice, hybrid models which implement both effects are geneally used in hydrodynamic simulations [30, 31]. The importance of the proton shape and its fluctuations to model the small system was recongnized in [31]. The hydrodynamics itself might not be the only mechanism of the observed collectivity was acknowledged in [32]. The influence and interplay of initial state and final state effects are recently studied carefully for the first time in [33], pointing out that the details of the initial state are crucially important for the quantitative description of observables in small systems [34]. The attempts to describe the collective effects systematically from the small to large systems are being made both for experiments [23] and theory side [33]. However, a quantitative description of the full set of experimental data has not yet been achieved. The summary of various explanations for the observed correlations in these small systems are summarized in [35].

Furthermore, if collectivity in small systems is due to final state interactions, it should be possible to measure its effect on jets. Proving the presence of jet quenching will be another crucial milestone to demonstrate the existence of the final-state effect in high multiplicity pp collisions. The most of observables for the jet quenching in pp and pPb collisions didn’t show any evidences so far []. The difficulties are attributed to an ambiguous reference since the hard probes themselves are also enhanced by requiring high multiplicity in the event [].

The ATLAS experiment has recently shown that the ridge remains in events tagged with a Z-boson [36], possibly with an accompanying jet. The impact paramenter dependence on di-jet or multi-jet production in pp collisons was studied in [37].  $v_2$  will be different. The microscopic model for collectivity, based on interacting string implemented in the PYTHIA8 Monte Carlo event generator so called “shoving

model” [38], can qualitatively reproduce the CMS near-side ridge yield [22] and ATLAS Z-tagged ridge. This challenges the hydrodynamic picture and predicts modifications to jet fragmentation properties [39].

To further investigate these effects, we studied long-range correlations as a function of transverse momentum in very high multiplicity pp collisions at  $\sqrt{s} = 13$  TeV, collected with the high multiplicity event trigger during 2016 and 2017 with ALICE. In this article, we present the near-side per-trigger yield at large pseudorapidity separation as a function of transverse momentum. The results are compared to previous measurements from CMS experiments. In addition, we present the ridge yield in events where harder fragmentation processes are present, to explore possible physical origins of long-range correlations. The experimental setup and measurements are described in Sec. 2. In Sec. 3 we present the analysis methods. The sources of systematic uncertainties are explained in Sec. 4. The results of the measurements are presented in Sec. 5. In Sec. 6 we present comparisons to model calculations. Finally, Sec. 7 summarizes our new results.

## 2 Experimental setup

Delivery of protons with world-highest energy by LHC at CERN makes it possible to generate various phenomena from their collisions. Recent center-of-mass energy of colliding two protons is increased up to  $\sqrt{s} = 13$  TeV during LHC Run2 period. Among data from proton-proton collisions at 13 TeV, This paper describes analysis results obtained by using 2016 to 2018 data sets. The full description of ALICE detector in the LHC Run 2 can be found in Ref. [?]. The present analysis mainly uses V0([?]), ITS (Inner Tracking System, [?]) and TPC (Time Projection Chamber, [?]) detectors.

The V0 detector consists of two rings, V0-A and V0-C, each made of 32 scintillator tiles, covering the full azimuthal angle within  $2.8 < \eta < 5.1$  and  $-3.7 < \eta < -1.7$ , respectively. The V0 provides trigger and estimation of event multiplicity. A sample of events including higher numbers of produced particles is obtained with a high multiplicity trigger, which is achieved by requiring higher amplitude of V0 Detector.

The responsibility of reconstruction of charged track is up to the ITS and the TPC. The ITS is composed of three subsystems, Silicon Pixel Detector (SPD), Silicon Drift Detector (SDD) and Silicon Strip Detector (SSD). The ITS has an acceptance up to  $|\eta| < 1.95$  for single charged track reconstruction. The TPC, which is working inside solenoidal magnetic field of 0.5 T, has an acceptance up to  $|\eta| < 0.9$  for charged tracks reaching the outer radius of the TPC. The tracking of charged-particles is done with the combination of the ITS and the TPC, which enable the reconstruction of tracks down to 0.2 GeV/c with  $\sim 75\%$  efficiency.

## 3 Analysis Procedure

The multiplicity class used in the present analysis is top 0-0.1%, which denotes the most particle-abundant events including  $\sim 31$  charged particles in the mid-rapidity region, to observe the clear ridge structure. This analysis uses charged particles, whose reconstructed transverse momenta are larger than 0.2 GeV/c in a fiducial region as  $|\eta| < 0.9$ . The efficiency and contamination from non-primary particles are estimated from a Monte Carlo simulation with PYTHIA8 event generator and with particle transport through the detector using GEANT simulation.

The two-particle correlation between trigger particle and associated particle is measured as function of relative pseudorapidity and azimuthal angle. The following equation expresses the correlation as associated yield per trigger particle as function of transverse momentum ( $p_{T,\text{trig}}, p_{T,\text{assoc}}$ ) of trigger particle and associated particle with the condition of  $p_{T,\text{trig}} > p_{T,\text{assoc}}$

$$\frac{1}{N_{\text{trig}}} \frac{d^2 N_{\text{pair}}}{d\Delta\eta d\Delta\phi} = B(0,0) \frac{S(\Delta\eta, \Delta\phi)}{B(\Delta\eta, \Delta\phi)}, \quad (1)$$

where the  $N_{\text{trig}}$  is the number of trigger particles in the corresponding event class. The signal distribution  $S(\Delta\eta, \Delta\phi)$  is constructed using two-particle correlation in the same event. The background distribution  $B(\Delta\eta, \Delta\phi)$  is constructed using two-particle correlation in mixed several events having the same primary vertex and belonging to the same multiplicity class.

The quantitative study of ridge is done with  $\Delta\phi$  distribution at large  $\Delta\eta$  to allow direct comparison of ridges between different  $p_T$  intervals. The large  $\Delta\eta$  range is defined as  $1.5 < |\Delta\eta| < 1.8$  considering the limited detector acceptance.

$$\frac{1}{N_{\text{trig}}} \frac{dN}{d\Delta\phi} = \int_{|\Delta\eta| > 1.5} d\Delta\eta \frac{1}{N_{\text{trig}}} \frac{d^2 N_{\text{pair}}}{d\Delta\eta d\Delta\phi} \quad (2)$$

The baseline of the correlations is subtracted by implementing Zero-Yield-At-Minimum (ZYAM) procedure. The minimum yield ( $C_{\text{ZYAM}}$ ) is defined as minimum value of the function, which consists of Fourier series up to the third harmonic and is determined by fitting the  $\Delta\phi$  distribution. By subtracting  $C_{\text{ZYAM}}$  from the  $\Delta\phi$  distribution, the magnitude of long-range near-side yield is obtained and can be quantified by integrating the near-side peak of the  $\Delta\phi$  distribution. The range of integration is enclosed by the points having the minimum yield, which is obtained from ZYAM procedure.

The ridge yield is further studied with various event selections regarding hard processes. The event selection is implemented by requiring that transverse momentum of leading track is larger than specific threshold. The leading track is defined as a charged track having the largest transverse momentum in a given event. Because the high transverse momentum track mainly comes from hard scattering, the requirement of the leading track can control the hardness of events, which allow one to study the ridge with events containing hard scatterings.

## 4 Systematic Uncertainty

The background distribution is constructed using several events having same primary vertex. The effect of construction of background distribution is estimated by varying the primary vertex interval from 2 cm to 1 cm. The estimated effect is 6-10%.

The  $\Delta\eta$  projection range for construction of long-range  $\Delta\phi$  is sensitive to contamination of non-flow effect. The effect of  $\Delta\eta$  projection range is estimated by varying the projection range. The estimated effect is 10-15% for  $p_T > 1.0$  GeV/c and 20% for  $0.5 < p_T < 1.0$  GeV/c.

The M.C. closure test for efficiency correction results in  $\sim 4\%$  discrepancy. The discrepancy is considered into systematic uncertainty.

The effect of primary vertex selection along the beam axis is estimated by varying the selection range of primary vertex from  $|z_{\text{vtx}}| < 8$  cm to  $|z_{\text{vtx}}| < 6$  cm. The estimated effect is  $\sim 4\%$ . The effect of rejection of pile-up events. is estimated by varying the methodology of pile-up rejection. The estimated effect is  $\sim 4\%$ . The effect of track selection is estimated by varying a few selection criteria included in track selection. The estimated effect is  $\sim 5\%$ .

**Table 1:** Summary of the systematic uncertainties. See text for details.

Source	Uncertainty
Event mixing	6-10%
$\Delta\eta$ projection range	10-15%
M.C. closure	4%
Primary vertex	4%
Pileup Cut	4%
Track selection	5%
Total	14-20%

## 5 Results

The two-dimensional associated yield per trigger particle is shown in Figure 1 for pairs of trigger particle and associated particle with  $1.0 < p_{T, \text{assoc}} < p_{T, \text{trig}} < 2.0$  GeV/c in pp collisions at  $\sqrt{s} = 13$  TeV in the 0-0.1% (left), 5-20% (middle) and 20-100% (right) multiplicity class estimated by V0 detector, which covers forward rapidity region. The ridge is clearly seen in high multiplicity class unlike in lower multiplicity classes.

The one-dimensional  $\Delta\phi$  distribution is shown in Figure 2 for pairs of particles with various  $p_T$  intervals in very high multiplicity class. The associated yield per trigger particle is compared with CMS results. The near-side peak is highest in the  $1.0 < p_T < 2.0$  interval and gradually decreases with increasing  $p_T$ .

The spectra of the ridge yield is shown in Figure 3 in very high multiplicity class and compared with CMS results. The estimator of particle multiplicity of ALICE is done with forward subsystem(V0), whereas that of CMS is done by mid-rapidity particles meeting with the condition of  $|\eta| < 2.4$  and  $p_T > 0.4$  GeV/c. Dedicated comparison is conducted and the difference of particle multiplicity is estimated to be about 20%. Taking into account the difference in acceptance of charged tracks and comparable definition of multiplicity,, the measurements are can be considered comparable with each other.

To further understand the behavior of the ridge in events including hard processes, the two-dimensional associated yield per trigger particle is measured with the leading track selection as shown in Figure 4. The ridge is still visible in the events where  $p_T^{\text{Lead}} > 7$  GeV/c, which means that the ridge co-exists with hard-scattering in pp collisions.

The one-dimensional  $\Delta\phi$  distribution with the leading track selection is shown in Figure 5. The near-side yield doesn't change with respect to the leading track requirements within the uncertainties, whereas the away-side peak increases as the leading track requirement gets stronger, presumably because of the increase of the recoil jet yield.

The ridge yield is inspected as a function of the leading track selection in Figure 6. As seen in the

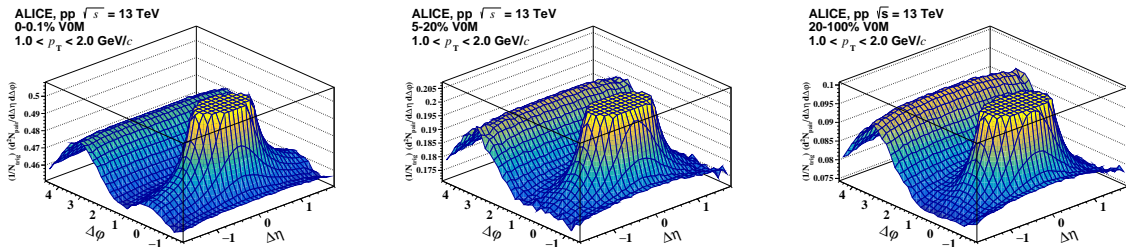


**Fig. 1:** Two-dimensional associated yield per trigger particle as function of  $\Delta\eta$  and  $\Delta\phi$  in 0-0.1% (left), 5-20% (middle) and 20-100% (right) multiplicity class. The interval of transverse momentum of trigger particle and associated particle is  $1.0 < p_T < 2.0$  GeV/c.

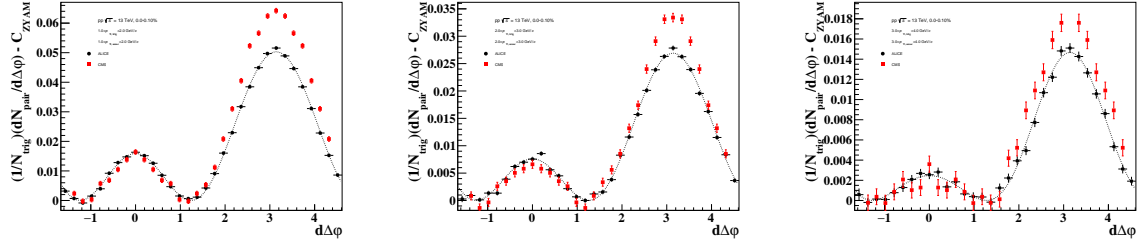


**Fig. 2:** One-dimensional  $\Delta\phi$  distribution in the large  $\Delta\eta$  with various transverse momentum intervals. Interval of transverse momentum of trigger particle and associated particle is  $1.0 < p_T < 2.0$  GeV/c (left),  $2.0 < p_T < 3.0$  GeV/c (middle) and  $3.0 < p_T < 4.0$  GeV/c (right), respectively.

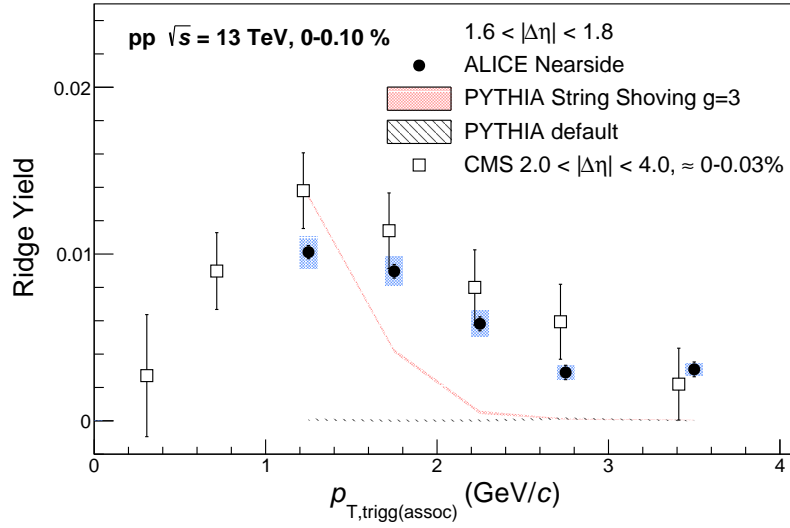


**Fig. 3:** (color online) The spectra of ridge yield as function of transverse momentum. The spectrum is compared with CMS result [? ].

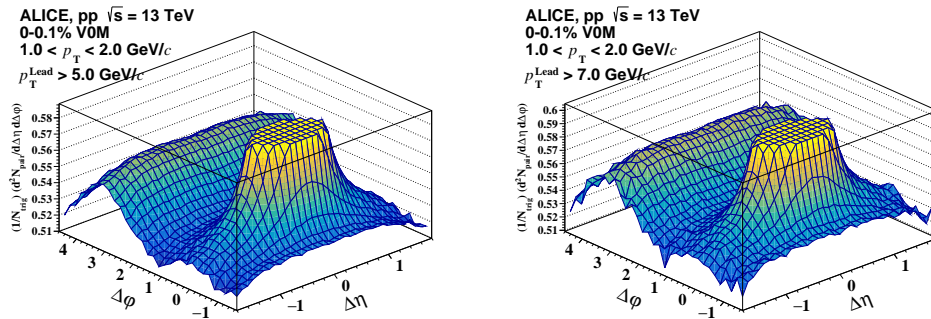


**Fig. 4:** Two-dimensional associated yield per trigger particle as function of  $\Delta\eta$  and  $\Delta\phi$  in top 0-0.1% multiplicity class. The interval of transverse momentum of trigger particle and associated particle is  $1.0 < p_T < 2.0$  GeV/c for the plots. Threshold for leading track selection is 5 GeV/c (left) and 7 GeV/c (right), respectively.

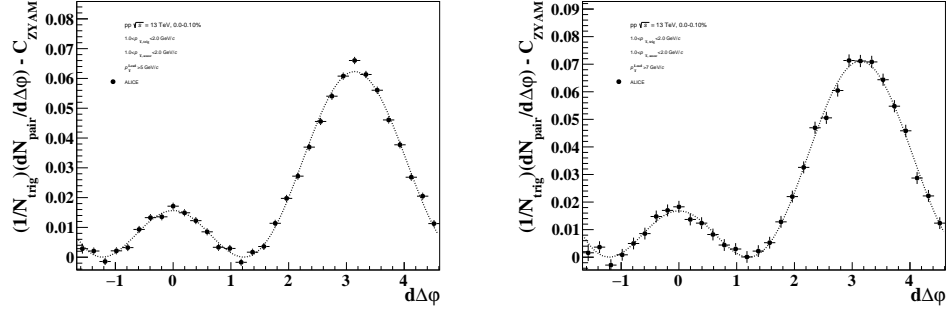


**Fig. 5:** One-dimensional  $\Delta\phi$  distribution in the large  $\Delta\eta$  with various leading track selection thresholds. Interval of transverse momentum of trigger particle and associated particle is  $1.0 < p_T < 2.0$  GeV/c. Threshold for leading track selection is 5 GeV/c (left) and 7 GeV/c (right) respectively.

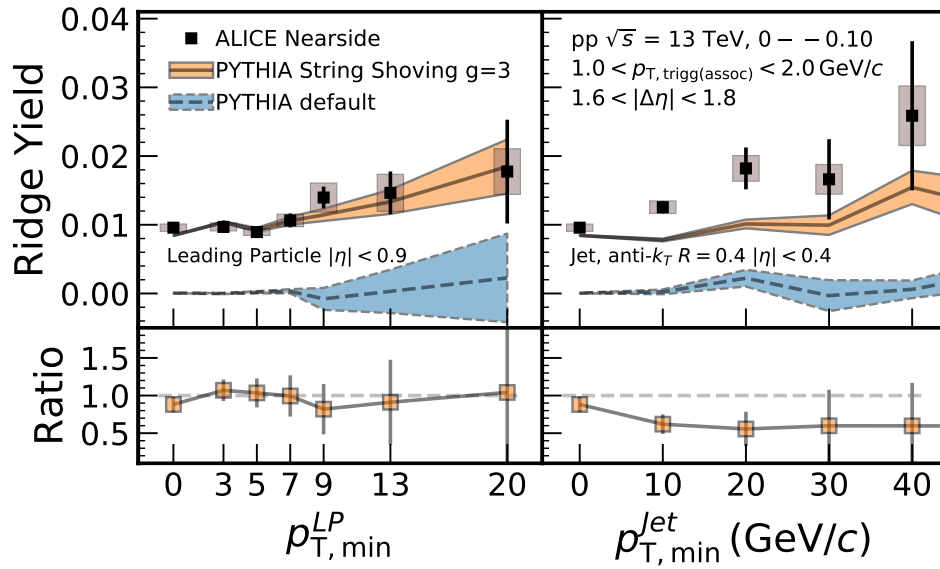


**Fig. 6:** The ridge yield spectrum with respect to the leading particle and jet selections. The ridge yields are identical within uncertainties.

previous plots, the ridge yield does not depend on the selection, which indicates that the ridge is not affected significantly by the hardness of the events.

## 6 Model Comparison

## 7 Conclusions

Two-particle angular correlations in large  $|\Delta\eta|$  has been measured in very high multiplicity events in pp collisions at  $\sqrt{s} = 13$  TeV with ALICE. The measured associated yield is found to be consistent with the previous results from CMS experiment. The ridge yield, for the first time, has been observed in events including hard processes. Furthermore, it is found to be independent of the hardness of the events. This observation is important for the study of the origins of the ridge in small collision systems.



## References

- [1] A. M. Poskanzer and S. A. Voloshin, “Methods for analyzing anisotropic flow in relativistic nuclear collisions,” *Phys. Rev.* **C58** (1998) 1671–1678, arXiv:nuc1-ex/9805001 [nuc1-ex].
- [2] S. A. Voloshin, A. M. Poskanzer, and R. Snellings, “Collective phenomena in non-central nuclear collisions,” arXiv:0809.2949 [nuc1-ex].
- [3] B. Alver and G. Roland, “Collision geometry fluctuations and triangular flow in heavy-ion collisions,” *Phys. Rev.* **C81** (2010) 054905, arXiv:1003.0194 [nuc1-th]. [Erratum: *Phys. Rev.* **C82**, 039903(2010)].
- [4] B. H. Alver, C. Gombeaud, M. Luzum, and J.-Y. Ollitrault, “Triangular flow in hydrodynamics and transport theory,” *Phys. Rev.* **C82** (2010) 034913, arXiv:1007.5469 [nuc1-th].
- [5] ALICE Collaboration, K. Aamodt *et al.*, “Higher harmonic anisotropic flow measurements of charged particles in Pb-Pb collisions at  $\sqrt{s_{NN}}=2.76$  TeV,” *Phys. Rev. Lett.* **107** (2011) 032301, arXiv:1105.3865 [nuc1-ex].
- [6] J. E. Bernhard, J. S. Moreland, S. A. Bass, J. Liu, and U. Heinz, “Applying Bayesian parameter estimation to relativistic heavy-ion collisions: simultaneous characterization of the initial state and quark-gluon plasma medium,” *Phys. Rev.* **C94** no. 2, (2016) 024907, arXiv:1605.03954 [nuc1-th].
- [7] J. E. Bernhard, J. S. Moreland, and S. A. Bass, “Bayesian estimation of the specific shear and bulk viscosity of quark-gluon plasma,” *Nature Physics* (2019) .  
<https://doi.org/10.1038/s41567-019-0611-8>.
- [8] STAR Collaboration, J. Adams *et al.*, “Experimental and theoretical challenges in the search for the quark gluon plasma: The STAR Collaboration’s critical assessment of the evidence from RHIC collisions,” *Nucl. Phys.* **A757** (2005) 102–183, arXiv:nuc1-ex/0501009 [nuc1-ex].
- [9] PHENIX Collaboration, K. Adcox *et al.*, “Formation of dense partonic matter in relativistic nucleus-nucleus collisions at RHIC: Experimental evaluation by the PHENIX collaboration,” *Nucl. Phys.* **A757** (2005) 184–283, arXiv:nuc1-ex/0410003 [nuc1-ex].
- [10] BRAHMS Collaboration, I. Arsene *et al.*, “Quark gluon plasma and color glass condensate at RHIC? The Perspective from the BRAHMS experiment,” *Nucl. Phys.* **A757** (2005) 1–27, arXiv:nuc1-ex/0410020 [nuc1-ex].
- [11] PHOBOS Collaboration, B. B. Back *et al.*, “The PHOBOS perspective on discoveries at RHIC,” *Nucl. Phys.* **A757** (2005) 28–101, arXiv:nuc1-ex/0410022 [nuc1-ex].
- [12] ALICE Collaboration, B. Abelev *et al.*, “Anisotropic flow of charged hadrons, pions and (anti-)protons measured at high transverse momentum in Pb-Pb collisions at  $\sqrt{s_{NN}}=2.76$  TeV,” *Phys. Lett.* **B719** (2013) 18–28, arXiv:1205.5761 [nuc1-ex].
- [13] ALICE Collaboration, B. B. Abelev *et al.*, “Elliptic flow of identified hadrons in Pb-Pb collisions at  $\sqrt{s_{NN}} = 2.76$  TeV,” *JHEP* **06** (2015) 190, arXiv:1405.4632 [nuc1-ex].
- [14] ATLAS Collaboration, G. Aad *et al.*, “Measurement of the pseudorapidity and transverse momentum dependence of the elliptic flow of charged particles in lead-lead collisions at  $\sqrt{s_{NN}} = 2.76$  TeV with the ATLAS detector,” *Phys. Lett. B* **707** (2012) 330–348, arXiv:1108.6018 [hep-ex].

- [15] P. Romatschke and U. Romatschke, “Viscosity Information from Relativistic Nuclear Collisions: How Perfect is the Fluid Observed at RHIC?,” *Phys. Rev. Lett.* **99** (2007) 172301, arXiv:0706.1522 [nucl-th].
- [16] ALICE Collaboration, J. Adam *et al.*, “Correlated event-by-event fluctuations of flow harmonics in Pb-Pb collisions at  $\sqrt{s_{NN}} = 2.76$  TeV,” *Phys. Rev. Lett.* **117** (2016) 182301, arXiv:1604.07663 [nucl-ex].
- [17] ALICE Collaboration, S. Acharya *et al.*, “Systematic studies of correlations between different order flow harmonics in Pb-Pb collisions at  $\sqrt{s_{NN}} = 2.76$  TeV,” *Phys. Rev.* **C97** no. 2, (2018) 024906, arXiv:1709.01127 [nucl-ex].
- [18] ALICE Collaboration, S. Acharya *et al.*, “Linear and non-linear flow modes in Pb-Pb collisions at  $\sqrt{s_{NN}} = 2.76$  TeV,” *Phys. Lett. B* **773** (2017) 68–80, arXiv:1705.04377 [nucl-ex].
- [19] ALICE Collaboration, S. Acharya *et al.*, “Linear and non-linear flow modes of charged hadrons in Pb-Pb collisions at  $\sqrt{s_{NN}} = 5.02$  TeV,” arXiv:2002.00633 [nucl-ex].
- [20] ATLAS Collaboration, G. Aad *et al.*, “Observation of Long-Range Elliptic Azimuthal Anisotropies in  $\sqrt{s} = 13$  and 2.76 TeV *pp* Collisions with the ATLAS Detector,” *Phys. Rev. Lett.* **116** no. 17, (2016) 172301, arXiv:1509.04776 [hep-ex].
- [21] CMS Collaboration, V. Khachatryan *et al.*, “Measurement of long-range near-side two-particle angular correlations in pp collisions at  $\sqrt{s} = 13$  TeV,” *Phys. Rev. Lett.* **116** no. 17, (2016) 172302, arXiv:1510.03068 [nucl-ex].
- [22] CMS Collaboration, V. Khachatryan *et al.*, “Evidence for collectivity in pp collisions at the LHC,” *Phys. Lett. B* **765** (2017) 193–220, arXiv:1606.06198 [nucl-ex].
- [23] ALICE Collaboration, S. Acharya *et al.*, “Investigations of Anisotropic Flow Using Multiparticle Azimuthal Correlations in pp, p-Pb, Xe-Xe, and Pb-Pb Collisions at the LHC,” *Phys. Rev. Lett.* **123** no. 14, (2019) 142301, arXiv:1903.01790 [nucl-ex].
- [24] ALICE Collaboration, B. Abelev *et al.*, “Long-range angular correlations on the near and away side in p-Pb collisions at  $\sqrt{s_{NN}} = 5.02$  TeV,” *Phys. Lett. B* **719** (2013) 29–41, arXiv:1212.2001 [nucl-ex].
- [25] X. Li, “Creation of quark-gluon plasma droplets with three distinct geometries,” *Nature Physics* **15** (03, 2019) .
- [26] K. Dusling and R. Venugopalan, “Evidence for BFKL and saturation dynamics from dihadron spectra at the LHC,” *Phys. Rev. D* **87** no. 5, (2013) 051502, arXiv:1210.3890 [hep-ph].
- [27] P. Sarma and B. Bhattacharjee, “Color reconnection as a possible mechanism of intermittency in the emission spectra of charged particles in PYTHIA-generated high-multiplicity *pp* collisions at energies available at the CERN Large Hadron Collider,” *Phys. Rev. C* **99** no. 3, (2019) 034901, arXiv:1902.09124 [hep-ph].
- [28] B. Arbuzov, E. Boos, and V. Savrin, “CMS ridge effect at LHC as a manifestation of bremsstrahlung of gluons due to the quark-anti-quark string formation,” *Eur. Phys. J. C* **71** (2011) 1730, arXiv:1104.1283 [hep-ph].
- [29] W. Zhao, Y. Zhou, H. Xu, W. Deng, and H. Song, “Hydrodynamic collectivity in proton–proton collisions at 13 TeV,” *Phys. Lett. B* **780** (2018) 495–500, arXiv:1801.00271 [nucl-th].

- [30] M. Greif, C. Greiner, B. Schenke, S. Schlichting, and Z. Xu, “Importance of initial and final state effects for azimuthal correlations in p+Pb collisions,” *Phys. Rev. D* **96** no. 9, (2017) 091504, arXiv:1708.02076 [hep-ph].
- [31] H. Mantysaari, B. Schenke, C. Shen, and P. Tribedy, “Imprints of fluctuating proton shapes on flow in proton-lead collisions at the LHC,” *Phys. Lett. B* **772** (2017) 681–686, arXiv:1705.03177 [nucl-th].
- [32] W. Zhao, Y. Zhou, K. Murase, and H. Song, “Searching for small droplets of hydrodynamic fluid in proton–proton collisions at the LHC,” arXiv:2001.06742 [nucl-th].
- [33] M. Greif, C. Greiner, B. Schenke, S. Schlichting, and Z. Xu, “Importance of initial and final state effects for azimuthal correlations in p+Pb collisions,” *Nucl. Phys. A* **982** (2019) 491–494, arXiv:1903.00314 [nucl-th].
- [34] B. Schenke, C. Shen, and P. Tribedy, “Hybrid Color Glass Condensate and hydrodynamic description of the Relativistic Heavy Ion Collider small system scan,” *Phys. Lett. B* **803** (2020) 135322, arXiv:1908.06212 [nucl-th].
- [35] M. Strickland, “Small system studies: A theory overview,” *Nucl. Phys. A* **982** (2019) 92–98, arXiv:1807.07191 [nucl-th].
- [36] **ATLAS** Collaboration, M. Aaboud *et al.*, “Measurement of long-range two-particle azimuthal correlations in Z-boson tagged  $pp$  collisions at  $\sqrt{s}=8$  and 13 TeV,” *Eur. Phys. J. C* **80** no. 1, (2020) 64, arXiv:1906.08290 [nucl-ex].
- [37] L. Frankfurt, M. Strikman, and C. Weiss, “Dijet production as a centrality trigger for  $pp$  collisions at CERN LHC,” *Phys. Rev. D* **69** (2004) 114010, arXiv:hep-ph/0311231.
- [38] C. Bierlich, G. Gustafson, and L. Lönnblad, “Collectivity without plasma in hadronic collisions,” *Phys. Lett. B* **779** (2018) 58–63, arXiv:1710.09725 [hep-ph].
- [39] C. Bierlich, “Soft modifications to jet fragmentation in high energy proton–proton collisions,” *Phys. Lett. B* **795** (2019) 194–199, arXiv:1901.07447 [hep-ph].